

IceCube - the next generation neutrino telescope at the South Pole

A. Karle for the IceCube Collaboration:

J. Ahrens^a, J.N. Bahcall^b, X. Bai^c, T. Becka^a, K.-H. Becker^d, D.Z. Besson^e, D. Berley^f, E. Bernardini^g, D. Bertrand^h, F. Binon^h, A. Biron^g, S. Böser^g, C. Boehm, O. Botnerⁱ, O. Bouhali^h, Th. Burgess^j, T. Castermans^k, D. Chirkin^l, J. Conrad^l, J. Cooley^m, D.F. Cowenⁿ, A. Davourⁱ, C. De Clercq^o, T. DeYoung^{m*}, P. Desiati^m, J.-P. Dewulph^h, B. Dingus^m, R. Ellsworth^f, P.A. Evenson^c, A.R. Fazely^p, T. Feser^a, T.K. Gaisser^c, J. Gallagher, R. Ganugapati^m, A. Goldschmidt^q, J. Goodman^f, A. Hallgrenⁱ, F. Halzen^m, K. Hanson^m, R. Hardtke^m, T. Hauschildt^g, M. Hellwig^a, P. Herquet^k, G.C. Hill^m, P.O. Hulth^j, K. Hultqvist^j, S. Hundertmark^j, J. Jacobsen^q, G.S. Japaridze^r, A. Karle^m, L. Köpke^a, M. Kowalski^g, J.I. Lamoureux^q, H. Leich^g, M. Leuthold^g, P. Lindahl, I. Liubarsky^s, J. Madsen^t, P. Marciniewski^l, H.S. Matis^q, C.P. McParland^q, Y. Minaeva^j, P. Miočiniović^l, R. Morse^m, R. Nahnauer^g, T. Neunhoffer^a, P. Niessen^o, D.R. Nygren^q, H. Ogelman^m, Ph. Olbrechts^o, C. Pérez de los Heros^l, A.C. Pohl, P.B. Price^l, G.T. Przybylski^q, K. Rawlins^m, E. Resconi^g, W. Rhode^d, M. Ribordy^g, S. Richter^m, H.-G. Sander^a, T. Schmidt^g, D. Schneider^m, D. Seckel^c, M. Solarz^l, L. Sparke, G.M. Spiczak^t, C. Spiering^g, T. Stanev^c, D. Steele^m, P. Steffen^g, R.G. Stokstad^q, P. Sudhoff^g, K.-H. Sulanke^g, G.W. Sullivan^f, T. Summers^s, I. Taboada^u, L. Thollander^j, S. Tilav^c, C. Walck^j, C. Weinheimer^a, C.H. Wiebusch^{g†}, Ch. Wiedemann^j, R. Wischniewski^g, H. Wissing^g, K. Woschnagg^l, Sh. Yoshida^v

^aInstitute of Physics, University of Mainz, Staudinger Weg 7, D-55099 Mainz, Germany

^bInstitute for Advanced Study, Princeton, NJ 08540, USA

^cBartol Research Institute, University of Delaware, Newark, DE 19716, USA

^dFachbereich 8 Physik, BUGH Wuppertal, D-42097 Wuppertal, Germany

^eUniversity of Kansas, Lawrence, KS, USA

^fDept. of Physics, University of Maryland, College Park, MD 20742, USA

^gDESY-Zeuthen, D-15735 Zeuthen, Germany

^hUniversité Libre de Bruxelles, Science Faculty CP230, B-1050 Brussels, Belgium

ⁱDivision of High Energy Physics, Uppsala University, S-75121 Uppsala, Sweden

^jDept. of Physics, Stockholm University, SCFAB, SE-10691 Stockholm, Sweden

^kUniversity of Mons-Hainaut, 7000 Mons, Belgium

^lDept. of Physics, University of California, Berkeley, CA 94720, USA

^mDept. of Physics, University of Wisconsin, Madison, WI 53706, USA

ⁿDept. of Physics, Pennsylvania State University, University Park, PA 16802, USA

^oVrije Universiteit Brussel, Dienst ELEM, B-1050 Brussels, Belgium

^pDept. of Physics, Southern University and A&M College, Baton Rouge, LA 70813, USA

^qLawrence Berkeley National Laboratory, Berkeley, CA 94720, USA

^rCTSPS, Clark-Atlanta University, Atlanta, GA 30314, USA

^sImperial College London, Exhibition Road, London SW7 2AZ, UK

^tPhysics Dept., University of Wisconsin, River Falls, WI 54022, USA

^uDepartamento de Física, Universidad Simón Bolívar, Apdo. Postal 89000, Caracas, Venezuela

^vDept. of Physics, Faculty of Science, Chiba University, Chiba 263-8522, Japan

IceCube is a large neutrino telescope of the next generation to be constructed in the Antarctic Ice Sheet near the South Pole. We present the conceptual design and the sensitivity of the IceCube detector to predicted fluxes of neutrinos, both atmospheric and extra-terrestrial. A complete simulation of the detector design has been used to study the detector's capability to search for neutrinos from sources such as active galaxies, and gamma-ray bursts.

1. INTRODUCTION

The successful deployment and operation of the AMANDA detector have shown that the Antarctic Ice sheet is an ideal medium and location for a large neutrino telescope. The detection of atmospheric neutrinos in agreement with expectations [2, 1] established AMANDA as a neutrino telescope. Searches for neutrinos from Supernova [3], dark matter [6], point sources of muon neutrinos [4] and diffuse sources of high energy electron [5] and muon neutrinos [7] have demonstrated the physics potential of a deep ice neutrino detector. However, a much larger detector is needed to reach a sensitivity required for the detection of many predicted neutrino fluxes. Current and proposed detectors at sites in the northern hemisphere are discussed in [9]. IceCube is a projected under ice neutrino detector consisting of 4800 PMT on 80 strings distributed over an area of 1 km^2 (figure 1) and instrumented at a depth between 1400 m and 2400 m. Detailed documentation can be found in [10]. A surface airshower detector consisting of 160 stations over 1 km^2 augments the deep ice component by providing a tool for calibration, background rejection and air shower physics. The Monte-Carlo simulation tools used to determine and optimize the performance of IceCube are verified with AMANDA data. They correctly describe the cosmic ray muon flux and the atmospheric neutrino flux [1].

One of the principal objectives of IceCube is the detection of sources of high energy neutrinos of astrophysical origin. IceCube is sensitive to all neutrino flavors over a wide range of energies. Muons can be observed from about 10^{11} eV to 10^{18} eV and beyond. Cascades, generated by ν_e , $\bar{\nu}_e$, ν_τ , and $\bar{\nu}_\tau$ can be observed and reconstructed at energies above 10^{13} eV . Tau events can be identified above energies of about a PeV. Interaction with the Earth will modulate the neutrino fluxes emerging at an underground detector.

The potential backgrounds of large under-

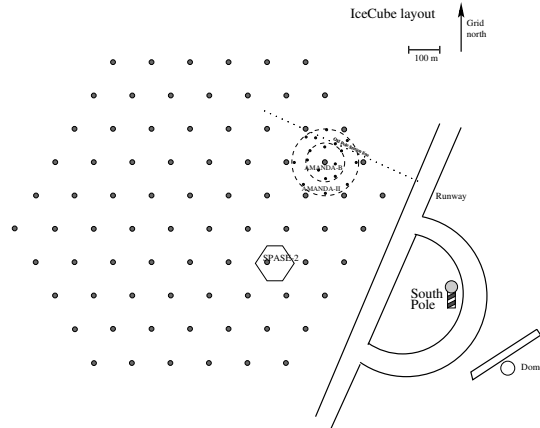


Figure 1. Schematic diagram of the arrangement of the strings of the IceCube detector at the South Pole station. The existing AMANDA detector and the SPASE air shower array will be embedded in the IceCube array.

ground detectors are downgoing cosmic ray muons, atmospheric neutrinos, and the dark noise signals detected in photomultipliers. The simulated trigger rate of downgoing cosmic ray muons in IceCube is 1700 Hz while the rate of atmospheric neutrinos (ν_μ and $\bar{\nu}_\mu$) at trigger level is about 300/day. Depending on the type of signal to be searched for this background is rejected using direction, energy, and neutrino flavor. At energies below $\approx 1 \text{ PeV}$, neutrino astronomy must focus on upward going neutrinos. At energies above 1 PeV, the cosmic ray muon background disappears while the low energy cosmic ray background can be rejected using an energy rejection cut. The background contribution from dark noise is not significant because the total dark noise rate of the optical sensor in situ is expected to be less than 0.5 kHz.

The highest sensitivity for astrophysical point sources can be achieved with muons. The muon channel stands out for two reasons. 1.) Muons allow a very good angular resolution of 0.7° over a wide energy range. 2.) The effective volume for muons exceeds the geometric volume of the detector by factors of 10 to more than 50 depending on energy. Due to the long range of high energy

*Present addr.: Santa Cruz Institute for Particle Physics, Univ. of Cal., Santa Cruz, CA 95064, USA.

†Present address: CERN, CH-1211, Genève 23, Switzerland.

muons the interaction of the ν_μ can take place at distances of tens of kilometers outside of the detector. We will focus on the muon detection because it provides the benchmark sensitivity for some of the fundamental goals of high energy neutrino astronomy.

2. DETECTOR DESIGN

The detector consists of 4800 photomultipliers arranged on 80 strings at depths of 1400 to 2400m. The strings are arranged in a regular spaced grid covering a surface area of 1 km^2 as shown in figure 1. A surface component of 160 ice Cherenkov tanks provides a detector for air showers with an energy threshold of about 1 PeV. Each string consists of a 60 optical modules (OM) spaced at 17m. The geometric arrangement and the total number of OM and strings is a result of MonteCarlo simulations with a variety of different geometries. The photomultiplier signals will be digitized inside the pressure housing [11]. The digitized signals are given a global time stamp with a precision of $<5\text{ ns}$ and transmitted to the surface. The digital messages are sent to a string processor, a global event trigger and event builder. All time calibrations will be automated. The geometry of the detector will be known to a precision of better than 2m initially after the deployment. It will be calibrated more precisely ($< 1\text{ m}$) with light flashers on board the OM and with cosmic ray muons. Both methods have been applied successfully in AMANDA. High energy signals and complex events can be calibrated with powerful lasers deployed with the detector. The absolute orientation can be calibrated with coincidences with the surface air shower component, IceTop, and over longer time scales, with the observations of the shadow of the moon. Once events are built in the surface DAQ, data will be processed and filtered. A reduced data set will be sent to the Northern hemisphere for further processing and data analysis on a daily basis. Twenty four hour satellite connectivity will be available for important messages. Construction of the detector is expected to commence in the Austral summer of 2004/2005 and continue for 6 years. The growing detector will be in operation dur-

ing construction, with each string coming online within days after deployment.

3. FUNDAMENTAL PERFORMANCE PARAMETERS

In detailed simulations we compared the response of the detector to cosmic ray muons, to atmospheric neutrinos and to a hypothetical hard neutrino spectrum as generated by a shock acceleration mechanism [12]. The event rates generated by all three fluxes, normalized to one year of on-time, are listed in table 1. The event rates are given at trigger level (minimum of 5 OM signals within a section of a string) and for full event reconstruction with cuts applied for the rejection of the cosmic ray muon background, which we refer to as “level 2”. Unless specified otherwise, basic background rejection cuts (level 2) are applied for all results shown. With an assumed flux strength of $E_\nu^2 \times dN_\nu/dE_\nu = 10^{-7}\text{ s}^{-1}\text{ cm}^{-2}\text{ sr}^{-1}\text{ GeV}$ for cosmic neutrinos, a factor of 10 below the current best limit to high energy diffuse neutrinos [7], we expect more than 1000 signal events. At this stage, both, the background from atmospheric neutrinos and the background from cosmic ray muons amount to roughly 10^5 events atmospheric neutrino induced muon events is based on [21]), including about 5000 events attributed to prompt decays of charmed mesons [18]. The application of an energy cut will quickly suppress remaining cosmic ray muon background.

	Trigger	Level 2
Cosmic ν	3.3×10^3	1.1×10^3
Atm ν	8.2×10^5	9.6×10^4
Atmosph. μ	4.1×10^{10}	10×10^4

Table 1

Event rates are given for 1 year of signal and background. The signal expectation corresponds to a source flux of $E_\nu^2 \times dN_\nu/dE_\nu = 10^{-7}\text{ s}^{-1}\text{ cm}^{-2}\text{ sr}^{-1}\text{ GeV}$. The expectation for atmospheric neutrino induced muon events is based on [21]) and it includes the prompt component according to [18](rqpmm).

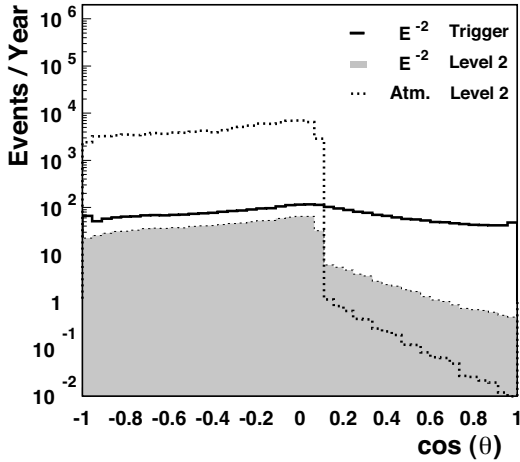


Figure 2. Distribution of the reconstructed zenith angle a) Signal from a E^{-2} -source at trigger level, b) with background rejection (level 2, shaded), and c) atmospheric neutrino background at level 2. Event numbers are normalized to one year.

Figure 2 shows reconstructed zenith angle distributions of atmospheric neutrinos and of the injected cosmic neutrino flux. Downgoing atmospheric neutrinos are highly suppressed at the level because low energy cosmic ray muons need to be rejected with energy cuts. The zenith angle distribution of the astrophysical neutrino spectrum is modified little below the horizon. Above the horizon the losses are much smaller than for atmospheric neutrinos because of the harder spectrum. However, no energy cut has yet been applied yet to upgoing muons.

3.1. Effective Detector Area

The detector sensitivity can be expressed in several quantities. One possible choice is the “effective detector area”. It is defined as

$$A_{\text{eff}}(E_{\mu}, \Theta_{\mu}) = \frac{N_{\text{detected}}(E_{\mu}, \Theta_{\mu})}{N_{\text{generated}}(E_{\mu}, \Theta_{\mu})} \times A_{\text{gen}}, \quad (1)$$

where $N_{\text{generated}}$ is the number of muons in the test sample that have an energy E_{μ} at any point within the fiducial volume and an incident zenith angle Θ_{μ} . We take the point of closest approach to the detector center (which might also lie out-

side the geometrical detector volume) for the energy dependency. N_{detected} is the number of such events that are triggered or pass the cut level under consideration.

The effective trigger area reaches one square kilometer at an energy of a few hundred GeV. Roughly 50% of all triggered events pass the “standard selection” (Level 2), independent of the muon energy. Figure 3 shows the effective areas for four separate energy ranges as a function of the zenith angle of the incident muon tracks. The detector will provide an effective detection area of one square kilometer for upward moving muons in the TeV range. Above 100 TeV the selection allows for a detection of downgoing neutrinos, *i.e.* for an observation of the southern hemisphere ($\cos\theta > 0$). In the PeV range the effective area for downgoing muons is above 0.6 km², increasing towards the horizon. This means that IceCube can be operated as a full sky observatory for PeV to EeV neutrinos.

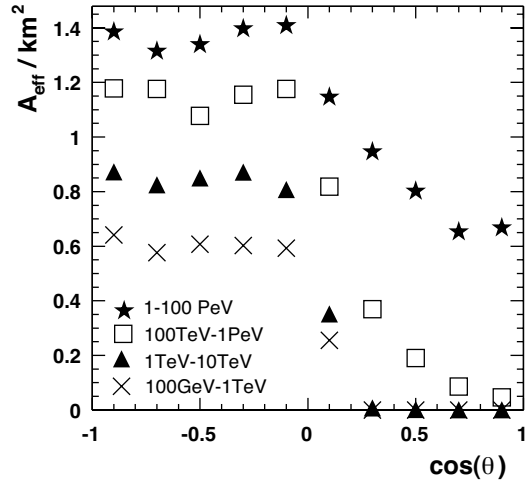


Figure 3. The effective area is shown as a function of the zenith angle after applying Level 2 cuts for four ranges of energy.

3.1.1. Angular resolution

The angular resolution of the detector is an important quantity for the search for neutrinos from point sources. Using the angular resolution

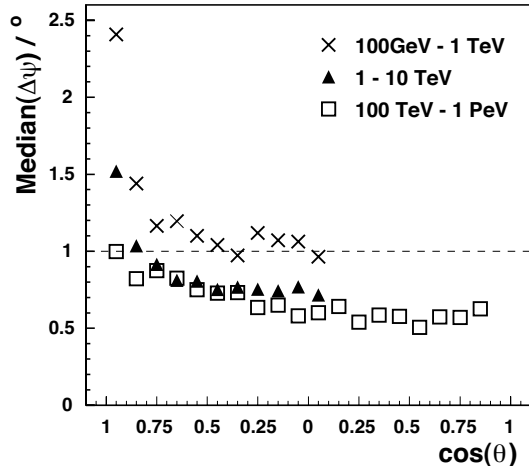


Figure 4. Pointing resolution for muons. Shown is the median space angle error of the reconstructed direction as a function of the zenith angle of the incident track.

of the detector, background events can be more easily eliminated by restricting the search to a small angular region about the known direction of the object under investigation. The median angular resolution (median pointing error) at different zenith angles is shown in figure 4.

The angular resolution is about 0.7° at TeV energies and approaches 0.6° near the horizon. We expect significant improvement of the pointing resolution with further development of the reconstruction algorithms, in particular from including amplitude or waveform information.

4. SENSITIVITY TO ASTROPHYSICAL NEUTRINO FLUXES

4.1. Diffuse fluxes

Theoretical models of astrophysical fluxes of high energy neutrinos are often linked to the known flux of very high energy cosmic rays, which are believed to be of extragalactic origin, see for example [13, 15, 16, 17]. Many models have been developed that predict the expected flux of neutrinos from the sum of all active galaxies in the universe. First we will consider the sensitivity of IceCube to detect a generic diffuse flux following

an E^{-2} spectrum. The harder energy spectrum of an astrophysical neutrino flux can be used to discriminate the atmospheric neutrino spectrum from the signal. We use a very simple and robust observable, the number of optical modules which have seen at least one photon, called the channel multiplicity (N_{ch}), as an energy separation cut. Atmospheric neutrino induced events have typical channel multiplicities (event sizes) of about 30 to 60 channels. The assumed high energy signal flux dominates the atmospheric neutrino background above channel multiplicities of about 200.

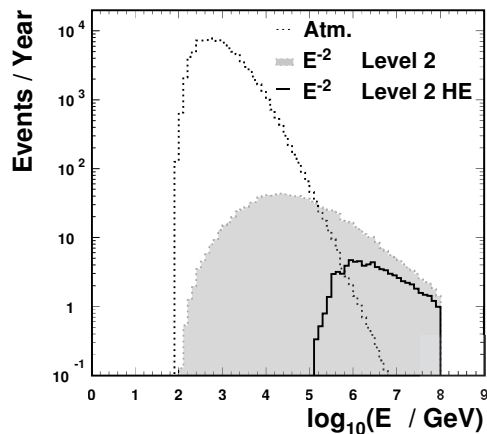


Figure 5. Energy spectra of detected neutrinos for a hypothetical E^{-2} source before (shaded) and after energy cut (solid line), and atmospheric neutrinos before the energy cut (dashed).

The simulated source strength of $E_\nu^2 \times dN_\nu/dE_\nu = 1 \times 10^{-7} \text{ s}^{-1} \text{ cm}^{-2} \text{ sr}^{-1} \text{ GeV}$ would result in an expectation of 74 signal events in one year of operation, compared to 8 background events from atmospheric neutrinos, after applying an optimal energy cut ($N_{\text{ch}} > 227$). The background expectation was calculated using the prompt charm prediction of Bugaev *et al.* [18], according to which, prompt decays of charmed mesons contribute 80% to the final atmospheric sample. After three years of operation an overall flux limit of $E^2 \times dN_\nu/dE_\nu =$

$4.2 \times 10^{-9} \text{ s}^{-1} \text{ cm}^{-2} \text{ sr}^{-1} \text{ GeV}$ is obtained. This is more than two orders of magnitude below the current limit obtained with AMANDA. This sensitivity would improve by a factor of 2 when using the charm prediction of TIG [19]. It should be noted that the sensitivity for diffuse ν_{e^-} and ν_{τ^-} fluxes may improve the overall sensitivity significantly. The energy spectra of the incident signal and background neutrinos are shown in figure 5. The applied energy cut results in an detection threshold of about 200 TeV. The sensitivity obtained after one year of data taking is already well below the Waxmann and Bahcall diffuse bound [14].

Apart from the generic case of a E^{-2} spectrum, which is typical for scenarios that involve meson production in interactions of Fermi accelerated cosmic rays with matter, we give the sensitivity to two other examples of diffuse models. Mannheim, Protheroe and Rachen have calculated an upper bound on the diffuse neutrino flux arising from photohadronic interactions in unresolved AGN jets in the universe. Their flux bound is shown in figure 6 labeled **MPR**, as a function of energy. Also shown is a model by Stecker and Salamon [17] for proton interactions on the UV thermal photon field in AGN cores, labeled **S&S**. When testing the sensitivity of IceCube to these specific models we found that IceCube would be sensitive to a flux of 2% of the **MPR** flux, and $2.3 \cdot 10^{-3}$ of the Stecker/Salamon flux. Also shown is the GRB flux prediction by Waxmann and Bahcall [15] (dash-dotted line). Here, the sensitivity limit, defined as a potential exclusion at 90% C.L., was calculated for an observation of 500 bursts (expectation for one year) in the northern sky (see section 4.3).

4.2. Sensitivity to Point Sources

An excess of events from a particular direction in the sky indicates the existence of a point source. The angular resolution of 0.7° allows using a search window of one degree radius that greatly reduces the background, while retaining a large fraction of the signal. In order to reject the remaining small number of atmospheric neutrinos we add a soft energy cut by requiring a channel multiplicity of $N_{\text{ch}}=30$. The ap-

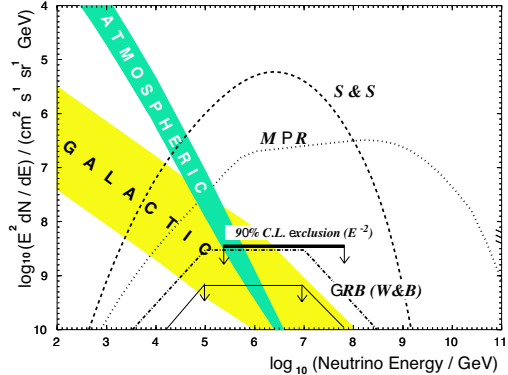


Figure 6. Expected sensitivity of the IceCube detector. The thick solid line indicates the 90% c.l. limit setting potential for an E^{-2} type spectrum for a time period of three years (see text for details). The thin solid line illustrates the GRB sensitivity for the reference spectrum [15].

plied energy cut suppresses atmospheric neutrinos of energies mostly below 1 TeV allowing an essentially background free detection potential for point sources. With these parameters we find an average flux upper limit of $E_\nu^2 \times dN_\nu/dE_\nu = 5.5 \times 10^{-9} \text{ s}^{-1} \text{ cm}^{-2} \text{ GeV}$ after one year of data taking. After five years of operation the sensitivity level would reach $E^2 \times dN_\nu/dE_\nu \sim 1.7 \times 10^{-9} \text{ s}^{-1} \text{ cm}^{-2} \text{ GeV}$.

4.3. Gamma Ray Burst Sensitivity

The origin of the high-energy gamma-ray burst emissions seen by orbiting satellites is still undetermined. If the acceleration mechanisms in these objects involve hadronic processes then the observed fluxes of gamma-rays should be accompanied by neutrinos. The detection of these neutrinos is made easier by using the time stamp and direction provided by the satellite observation. This small duration of gamma ray bursts allows for an essentially background-free search opportunity. Waxman and Bahcall [15] calculated the expected flux of neutrinos from the sum of all gamma-ray bursts by assuming that the acceleration mechanism is hadronic and is responsible for the observed flux of cosmic rays. The en-

ergy spectrum predicted by Waxman and Bahcall is shown in figure 6. A diffuse search for gamma-ray bursts involves summing over the observation time and spatial search windows for many separate bursts.

We considered at the moment an observation only over the northern sky, where the search will not be limited to higher energies due to downgoing CR muon background. A downgoing search would be similar, only it would require a harder energy cut. From the remaining rate of 500 bursts per 2π sr and year we would expect 13 neutrino induced up-going muons at 0.1 background events. For this analysis we used a hypothetical observation duration of 10 seconds and a spatial search cone of 10° centered about the direction of the GRB. The upper limit to the associated GRB flux would be 20% of the flux calculated by Waxmann and Bahcall.

5. OTHER SCIENCE OPPORTUNITIES

5.1. Dark matter

If Weakly Interacting Massive Particles (WIMPs) make up the dark matter of the universe, they would also populate the galactic halo of our own Galaxy. They would get captured by the Earth or the sun where they would annihilate pairwise, producing high-energy muon neutrinos that can be searched for by neutrino telescopes. A favorite WIMP candidate is the lightest neutralino which arises in the Minimal Supersymmetric Model (MSSM). The typical energy of the neutrino-induced muons would be of the order of $\approx 25\%$ of the neutralino mass. The predicted muon rates from WIMPs annihilating in the Sun range up to $10^4 km^{-2}$ per year at $\approx 100 GeV$ and more than a $10^4 km^{-2}$ up to energies of $\approx 1 TeV$. Current limits lie at fluxes of several thousand events at energies above 100 GeV. Simulations indicate that IceCube should reach sensitivities below 50 muon events per year for WIMPs from the sun [20]. Analysis methods for WIMP searches be optimized for low energies. IceCube could play a complementary role to future direct detection experiments (like CRESST or GENIUS) for annihilation in the Earth, and may even have a slight advantage over direct de-

tection experiments for certain low-mass WIMP models and annihilation in the Sun.

5.2. Cosmic rays and airshowers

Combined with the $1 km^2$ surface detector IceCube can do unique coincidence and anti-coincidence measurements with high energy air showers. In addition to providing a sample of events for calibration and for study of air-shower-induced backgrounds in IceCube, the surface array will act as a partial veto. All events generated by showers with $E > 10^{15}$ eV can be vetoed when the shower passes through the surface array. In addition, higher energy events, which are a potential source of background for neutrino-induced cascades, can be vetoed even by showers passing a long distance outside the array. The IceCube-IceTop coincidence data will cover the energy range from below the knee of the cosmic-ray spectrum to $> 10^{18}$ eV. Each event will contain a measure of the shower size at the surface and a signal from the deep detector produced by muons with $E > 300 GeV$ at production. At the high elevation of the South Pole, showers will be observed near maximum so that measured shower size provides a good measure of the total shower size. The combined measurement of the muon-induced signal in IceCube and the shower size at the surface will give a new measure of primary composition over three orders of magnitude in energy. In particular, if the knee is due to a steepening of the rigidity spectrum, a steepening of the spectrum of protons around $3 \cdot 10^{15}$ eV should be followed by a break in the spectrum of iron at $8 \cdot 10^{16}$ eV. The method to measure the composition has been developed and applied successfully with AMANDA and the surface airshower array SPASE-2 [22].

5.3. SUPERNOVAE

Although the MeV-level energies of supernova neutrinos are far below the AMANDA/IceCube trigger threshold, a supernova could be detected by observing higher counting rates of individual PMTs over a time window of 5-10 s. The enhancement in rate of one PMT will be buried in dark noise signals of that PMT. However, summing the signals from all PMTs over 10 s, signifi-

cant excesses can be observed. With background rates more than 10 times lower than ocean experiments, IceCube has the potential to see a supernova and to generate an alarm signal.

5.4. Cascades and very high energies

Due to its large and regularly instrumented volume, IceCube has a high sensitivity for cascades generated by ν_e , $\bar{\nu}_e$, ν_τ , and $\bar{\nu}_\tau$. Cascades have a superior energy resolution because all energy is deposited on a small volume of ≈ 10 metres diameter, and the amount of Cherenkov photons scales linearly with the deposited energy. At energies above a few tens of TeV the detector becomes fully efficient to cascade detection with an effective volume comparable to the geometric volume of 1 km³. At energies above 1 PeV chances increase to distinguish tau events from the ν_e -induced cascades. Extremely energetic muon events reach effective areas well beyond the geometric area as indicated in figure 3. Effective areas at 10¹⁸ eV are estimated to reach more than 2.5 km². Reconstruction algorithms for the more complex event topologies such as from tau events and for extreme energies beyond 10¹⁸ eV are not developed yet. However, the high resolution and high dynamic range data acquisition system of IceCube will provide rich information to extract the physics from such events.

6. ACKNOWLEDGEMENTS

This material is based upon work supported by the following agencies: The U.S. National Science Foundation under Grant Nos. OPP-9980474 and OPP-0236449; University of Wisconsin Alumni Research Foundation; U.S. Department of Energy; Swedish Research Council; Swedish Polar Research Secretariat; Knut and Alice Wallenberg Foundation, Sweden; Federal Ministry for Education and Research (Germany); U.S. National Energy Research Scientific Computing Center (supported by the Office of Energy Research of the U.S. Department of Energy); Deutsche Forschungsgemeinschaft (DFG).

REFERENCES

1. J. Ahrens *et al.* *Phys. Rev. D* **8007** (2002)
2. E. Andres *et al.* *Nature* **410**, 441-443 (22 March 2001)
3. J. Ahrens *et al.*, *Astropart.Phys.*16:345-359, 2002, astro-ph/0105460
4. J. Ahrens *et al.*, *subm. to Astroph. Journal.*
5. J. Ahrens *et al.*, Submitted to *Phys.Rev.D*, astro-ph/0206487.
6. Ahrens J. *et al.*, *Phys. Rev D*66, 032006 (2002), astro-ph/0202370.
7. G. C. Hill and M. Leuthold *Proc. 27th ICRC, Hamburg Germany* (2001)
8. D.F. Cowen for the AMANDA Collaboration, contributed talk, this conference.
9. G. Domogotsky for the Baikal Coll. and J. Carr, contrib. talks, this conference.
10. J. Ahrens *et al.*, The IceCube Proposal to NSF (2000), J. Ahrens *et al.*, PDD: IceCube Conceptual Design Document (2001), <http://icecube.wisc.edu>
11. R.G. Stokstad for the IceCube collaboration, this conference.
12. Sensitivity of the IceCube Detector to Astrophysical Sources of High Energy Muon Neutrinos, J. Ahrens *et al.*, to be published.
13. See, for example: T.K. Gaisser, F. Halzen and T. Stanev, *Phys. Rept.* 258 (1995) 173; J.G. Learned and K. Mannheim, *Ann. Rev. Nucl. Part. Sci.* 50 (2000) 679; V.S. Berezinsky and V.I. Dokuchaev, *Astropart. Phys.* 15 (2001) 87; A. Levinson and E. Waxman, *Phys. Rev. Lett.* 87 (2001) 1711101.01.
14. E. Waxman and J. Bahcall *Phys. Rev. D* 54 (1999) 023002
15. E. Waxman and J. Bahcall *Phys. Rev. D* 59 (1999) 023002
16. K. Mannheim, R.J. Protheroe and J.P. Rachen *Phys. Rev. D*63 (2000) 023003
17. F. W. Stecker and M. H. Salamon *Space Sci. Rev.* 75 341 355 (1996)
18. Bugaev *et al.* *em Phys. Rev. D* 58 (1998) 054001.
19. M. Thunman, G. Ingelman and P. Gondolo *Astropart.Phys.* **5** 309-332 (1996)
20. J. Edsjo, WIMP searches with IceCube, Amanda Internal report, Jan.7, 2000.
21. P. Lipari *Astropart. Phys* **1** 195-227 (1993)
22. K. Rawlins, 2001, Ph.D. Thesis, UW-Madison,

<http://amanda.physics.wisc.edu/Docs/>